Syd/JIP3 Controls Tissue Size by Regulating Diap1 Protein Turnover Downstream of Yorkie/YAP

Vakil Ahmad, Gangadhar P. Vadla, Chiswili Y. Chabu

University of Missouri, Division of Biological Sciences and the School of Medicine,

Columbia, Missouri 65211

Corresponding author: C.Y. Chabu (chabuc@missouri.edu)

Highlights

- Syd/JIP3 is required for proper *Drosophila* wing size
- Syd/JIP3 functions downstream of Yorkie by stabilizing Diap1 to promote cell survival during rapid tissue growth
- Yorkie-mediated tissue growth is highly sensitive to Syd/JIP3 dosage
- Syd/JIP3 is downregulated at the end of the tissue expansion phase

Abstract

How organisms control organ size is not fully understood. We found that Syd/JIP3 is required for proper wing size in Drosophila. *JIP3* mutations are associated with organ size defects in mammals.

Our mechanistic studies place Syd/JIP3 downstream of Hippo. Syd/JIP3 is dispensable for Hippo transcriptional activity but it is essential for Diap1 protein stability and function. Consistent with this observation, Syd/JIP3 inhibition reduces Diap1 protein levels and, correspondingly, elevates cell death in wing tissues. Partial restoration of Diap1 rescues wing size. In addition, Syd/JIP3 is upregulated in response to Yorkie activation. Importantly, Syd/JIP3 is required for the full effect of Yorkie-mediated tissue overgrowth. Thus, Syd/JIP3 is a novel organ size regulator in the Hippo pathway. This study provides mechanistic insights into the recent and perplexing link between *JIP3* mutations and organ size defects in mammals, including in humans where de novo *JIP3* variants are associated with microcephaly.

Introduction

The molecular basis of organ size regulation is a central question in developmental biology. Systemic signals such as insulin and growth factors play a key role in determining body and organ size. In *Drosophila*, starvation or genetic mutations in nutrient-sensing genes produce animals with smaller organs via well-defined and evolutionarily conserved mechanisms (Katsuyama et al., 2015; Stocker and Hafen, 2000). In addition to these systemic factors, transplantation experiments in salamander and in *Drosophila* have revealed that tissues possess intrinsic size control mechanisms. Salamander limbs maintain their size when transplanted onto animals with different limb sizes (Twitty V. C., 1931). Similarly, fragments of larval wing discs or young intact wings grow to reach normal size when transplanted into the abdomen of adult flies (Bryant and Levinson, 1985). In

contrast to systemic signals, these tissue-intrinsic organ size control mechanisms are not well understood.

The *Drosophila* wing imaginal disc is a powerful experimental system to understand growth control mechanisms. Embryonically derived cells undergo several rounds of cell proliferation to form a mature epithelium that ultimately gives rise to an adult wing with stereotyped size and shape (Day and Lawrence, 2000; Fristrom and Chihara, 1978; Garcia-Bellido, 1975; Garcia-Bellido and Merriam, 1971; Mandaravally Madhavan and Schneiderman, 1977; Martin et al., 2009; Milan et al., 1996; Worley et al., 2013). Genetic screens aimed at identifying mutations that deregulate growth in this system have led to the discovery of key and broadly conserved tissue-intrinsic growth control signaling pathways, including the Hippo pathway (reviewed in Hariharan, 2015; Irvine and Harvey, 2015; Pan, 2007). In fly and mammalian tissues, Hippo signaling potently controls tissue size by modulating the activity of Yorkie/YAP, a transcriptional co-activator for cell proliferation and cell survival genes (Dong et al., 2007; Huang et al., 2005; Jia et al., 2003; Oh and Irvine, 2008; Pan, 2007). An earlier study reported that the Jun NH-terminal kinase (JNK, also known as Bsk–FlyBase) regulates Hippo in the developing wing to control wing size. Localized JNK activity represses Hippo activity to promote cell proliferation throughout the tissue, hence promoting wing growth (Willsey et al., 2016). Hippo is a central tissue-size regulator, and its function is well conserved across species. While core signaling components of the Hippo pathway are well defined, downstream inhibitory mechanisms for restraining growth and achieving size stereotypy remain elusive (Pan, 2007).

Mitogen activating protein kinase (MAPK) scaffolding proteins mediate cellular responses to apoptotic or proliferative signals. Sunday Driver (Syd) or JNK-interacting protein-3 (JIP3) belongs to a family of conserved scaffolding proteins that bind to and facilitate JNK activation (Davis, 2000; Kelkar et al., 2000). Syd/JIP3 also regulates vesicle transport in worm and mammalian cells

(Caswell and Dickens, 2018; Choudhary et al., 2017; Edwards et al., 2013; Gowrishankar et al., 2017; Sun et al., 2017; Taylor and Alessi, 2020).

Using the developing *Drosophila* wing as a model system, we found that Syd/JIP3 is required for proper wing size. Mechanistic studies revealed that Syd/JIP3 functions downstream of Yorkie/YAP by controlling the stability of Diap1, an important cell survival regulator and Yorkie/YAP target. Syd/JIP3 regulates Diap1 post-transcriptionally by controlling its protein turnover. Congruent with these observations, knocking down Syd/JIP3 has no effect on Diap1 transcription but leads to a loss of Diap1 protein and correspondingly causes ectopic cell death, resulting in a reduced wing size. Restoring Diap1 protein in Syd/JIP3 knockdown tissues restores wing size. Importantly, activation of Yorkie/YAP upregulates Syd/JIP3 protein, and interfering with this stimulation suppresses Yorkie/YAP-mediated tissue overgrowth. In addition to defining a novel growth control mechanism, this work provides molecular insights into the perplexing association between *JIP3* mutations and small brains in mice and humans (Kelkar et al., 2003; Platzer et al., 2019).

Materials and Methods

Fly strains

All the crosses were maintained at 25°C unless otherwise described. Fly strains used for this study are: *UAS-Syd-RNAi* (Bloomington Stock #43232), *UAS-dSyd.GFP* (Mary K. Baylies), *Df(3L)syd*^{A2} (Bloomington Stock #32017), *syd*^{PL00426} (Bloomington Stock #19495), *UAS-Bsk-DN* (Tian Xu), *UAS-Yki* (Doujia Pan), *UAS-Hpo-RNAi* (Bloomington Stock #33614), *UAS-Diap1-RNAi* (Bloomington Stock #33597), *diap1-LacZ* (Bloomington Stock #12093), *diap1*$^{33\text{-}1s}$ (Hermann Steller), *fj-LacZ* (Bloomington Stock #44253), *CycE-lacZ* (Bloomington Stock #59065), *ex-lacZ* (Bloomington Stock #44248), *Jub-GFP* (Bloomington Stock #56806), *dronc*^{51} (Bloomington Stock

#23284), including GAL4 drivers *engrailed-Gal4*, *nubbin-Gal4*, *patched-Gal4*, *hedgehog-Gal4*, and *gmr-Gal4*.

Immunohistochemistry

Wind imaginal discs were dissected, fixed, and stained as previously described (Chabu and Xu, 2014; Pagliarini and Xu, 2003). The primary antibodies used are rabbit anti-PH3 (1:1000, Sigma), rat anti-Ci (1:500, Developmental Studies Hybridoma Bank, 2A1), rabbit anti-Diap1 (1:1000, Hermann Steller), rabbit anti-pWts (1:200, D. Pan), and mouse anti-β-gal (1:1000, Sigma). Secondary antibodies were from Invitrogen. Specimens were imaged on a Leica TCS SP8 confocal microscope. Images were analyzed and processed with IMARIS (Bitplane, Switzerland) and Adobe Illustrator software (Adobe).

Western blots

Wing imaginal discs from 75 wandering third-instar larvae carrying *hh-Gal4, UAS-srcRFP* (control) or *hh-Gal4, UAS-srcRFP, UAS-Syd-RNAi* (experimental) transgenes were dissected and homogenized in lysis buffer (50 mM HEPES pH 7.5, 150 mM KCl, 5 mM MgCl2, 0.01% Triton-X) supplemented with protease and phosphatase inhibitor cocktail (Cat #78443, Thermo Scientific). Proteins were electrophoresed on SDS-PAGE using 4-15% Mini-PROTEAN® TGX™ precast gel (Cat #456-1085, Bio-Rad), transferred onto nitrocellulose membranes, and incubated with rabbit anti-Diap1 (1:1000, Hermann Steller) and rabbit anti-β-Actin (1:1000, Cat #4967, Cell Signaling Technology) antibodies overnight. Anti-rabbit HRP-conjugated secondary antibodies (1:5000, Cat #31460, Invitrogen), ECL reagents (Cat #RPN2232, GE Healthcare), and the ChemiDoc™ MP Imaging System (Bio-Rad) were used to detect proteins.

For cell culture, protein lysates were prepared in lysis buffer (20 mM Tris-HCl pH-7.5, 150 mM NaCl, 1 mM Na2EDTA, 1 mM EGTA, 1% Triton, 2.5 mM sodium pyrophosphate, 1 mM β-

glycerophosphate, 1 mM Na3VO4, 1 μg/ml leupeptin) supplemented with protease and a phosphatase inhibitor cocktail (Cell Signaling #9803S). Proteins were electrophoresed on SDS-PAGE using 4-20% Mini-PROTEAN® TGX™ precast gel (Cat #456-1094, Bio-Rad), transferred onto PVDF membranes. PVDF membranes were incubated in blocking buffer (5% milk in Tris buffered saline, 0.1% Tween-20) at room temperature. Membranes were blotted overnight with anti-JIP-3 (1:1000, Cat #46663, Santa Cruz) or anti-GAPDH (1:1000, Cat #5174S, Cell signaling) antibodies at 4°C. Secondary antibodies used are anti-mouse horseradish peroxidase (HRP) (1:5000, Cat #31430, Invitrogen) and anti-rabbit HRP (1:15000, Cat #31460, Invitrogen). Protein bands were detected using the ECL kit (Cat #32106, Thermo Fisher scientific) and ChemiDoc™ MP Imaging System (Bio-Rad).

Adult wing imaging and measurements

Adult wings of female animals were dissected, mounted, flattened with a glass slide, and imaged using Leica Microsystems, DMC 4500. Areas of the adult wings were measured using the *freehand selection* and *analyze* tools of ImageJ software 1.50i. P-values were calculated using the two-tailed t-test function in Microsoft Excel.

Cell death detection in *Drosophila*

For labeling dead cells with TUNEL assay, the ApopTag® Red In Situ Apoptosis Detection Kit (Cat # S7165) was used according to the manufacturer's instructions. Briefly, dissected wing discs were fixed and incubated in an equilibration buffer at room temperature for 20 min followed by incubation with terminal deoxynucleotidy transferase in a reaction buffer for 1 h at 37°C. The reaction was stopped using a stop buffer diluted in dH_2O. Discs were incubated with conjugated anti-digoxigenin antibodies for 2 h at room temperature, washed, and mounted using a Vectashield mounting medium.

Cell lines and cell culture

Authenticated Human Embryonic Kidney 293 (HEK-293) cells were cultured in Dulbecco's Modified Eagle Medium (#11965-092) supplemented with 10% FBS. TrypLE (Gibco#12604-021) was used for immobilizing cells. Cells were counted in a Neubaur cell counter chamber following Trypan Blue dead cell exclusion (Cat #T8154, Sigma). Dharmacon on-target siRNA-SMARTpool plus Human scramble control (Cat #D-001810-10-05, Dharmacon) or JIP3 (Cat #L-003596-00-0005, Dharmacon) was used for RNA interference experiments in HEK-293 cells. DharmaFECT (Cat #T2002-02, Dharmacon) was used for transfection. Protein knockdown was assessed 72 hours after transfection.

Real-time RT-PCR

Drosophila wing tissues were dissected from 72-96 hours after egg-laying (AEL) or from 120-150 hours AEL wild-type animals for Syd/JIP3 real-time PCR (qRT-PCR). EZ Tissue/Cell culture total RNA Miniprep kit (Cat #R1002-50, Bio Research) was used to extract RNA in biological triplicates. The cDNA Reverse Transcription kit (Cat #4368814, Applied Biosystem) was used to generate cDNA from 100 ng total RNA. SYBR Green iTaq Supermix (Bio-Rad) was used for qRT-PCR. Expression of housekeeping gene *Rp49* (RpL32–FlyBase) was used as an internal control. Primer sequences are as follows:

Syd: 5'-ACTTGACTCTACGCTGCGGCTGT-3' and 5'-GGTGCCGATCCACAGCCGGT-3'

rp49: 5′-GGCCCAAGATCGTGAAGAAG-3′ and 5′-ATTTG-TGCGACAGCTTAGCATATC-3′

Flow cytometry analysis

Flow cytometric detection of the cell death dye propidium iodide (PI) was used. PI was used at 10 μg/ml in PBS containing 1% BSA. PI was detected at 488/636 nm (excitation/emission) on an ADP Beckman Coulter flow cytometer.

Statistical analysis

All *in vitro* experiments were reproducibly performed using biological triplicates. A student's *t-test* was used for comparing the difference between two groups, and a $p < 0.05$ was considered as statistically significant.

Results

Syd/JIP3 knockdown suppresses wing size independent of JNK

We knocked down Syd/JIP3 in the developing wing (*nubGAL4>Syd-RNAi*) and this resulted in smaller adult wings compared to controls (Figure 1A-E). Similarly, heterozygosity of two independent null alleles of *Syd* (Bowman et al., 2000; Hacker et al., 2003) ($syd^{PL00426/A2}$) yielded animals with smaller wings compared to controls (Figure 2F, K). Thus, Syd/JIP3 regulates *Drosophila* wing size. Interestingly, *jip3 loss of function* mutations are associated with brain size defects in mice and humans (Kelkar et al., 2003; Platzer et al., 2019). We sought to determine the mechanism by which Syd/JIP3 regulates tissue size.

The wing disc consists of a posterior (P) and an anterior (A) compartment. The patterning gene *engrailed* is specifically expressed in the P compartment of the wing disc where it induces Hedgehog (Hh) expression, while transcriptionally repressing Hh target genes (Garcia-Bellido, 1975; Tabata et al., 1992; Zecca et al., 1995). Hh protein is transported via cell-to-cell exocytosis-endocytosis cycles to the A compartment, where it activates Cubitus interuptus (Ci or Gli in vertebrates). In turn, Ci stimulates the expression of dTRAF1 (*Drosophila* tumor necrosis factor receptor-associated factor-1) a JNK pathway component, leading to JNK signaling activation at the P/A boundary. This localized JNK activity acts via the LIM domain family protein ajuba to repress Hippo signaling throughout the entire tissue (Sun and Irvine, 2013; Willsey et al., 2016). It is unclear how this local effect on Hippo signaling is transferred throughout the whole tissues to promote tissue growth.

We asked whether Syd/JIP3 regulates wing size via this Ci-JNK-Hippo signaling cascade. RNAi knockdown of Syd/JIP3 in the P/A boundary cells where JNK is normally active (*ptcGAL4>Syd-RNAi*) reduced wing size (Figure 2G, K), raising the possibility that Syd/JIP3 regulates wing via JNK.

To directly test this hypothesis, we performed genetic epistasis experiments between Syd/JIP3 and JNK. We used the P/A boundary driver *ptcGAL4* to express a potent JNK inhibitor (dominant-negative version of JNK, *Bsk-DN*) alone or in the presence of *Syd-RNAi* and the determined the effect of these manipulations on adult wing size. As expected, *Bsk-DN* reduced wing size compared to control (Figure 2H, K). This size reduction effect was not as pronounced as what we had observed with *Syd-RNAi* knockdown at the P/A boundary or throughout the wing tissue (*nubGAL4, Syd-RNAi*) (Figure 1A-E and Figure 2G, H, K). Importantly, blocking JNK failed to exacerbate the small wing phenotype caused by Syd knockdown (*ptcGAL4>Bsk-DN, Syd-RNAi*). Instead, these wings resembled Syd-depleted wings (Figure 2G-I, K). Moreover, overexpression of wild-type version of *Syd* rescued the *Bsk-DN* small wing phenotype (Figure 2H, J, K). Collectively, these findings argue that Syd/JIP3 is epistatic to JNK and that Syd/JIP3 functions downstream of JNK.

JNK acts via the LIM domain family protein Ajuba to repress Hippo signaling and promotes wing growth (Willsey et al., 2016). Ajuba represses Hippo by sequestering Warts, a negative regulator of Yorkie/YAP, to cell-cell junctions. This sequestration increases Yorkie/YAP activity, which transcriptionally stimulates CyclinE and the E3-ubiquitin ligase *Drosophila* inhibitor of apoptosis (Diap1) to simultaneously promote cell proliferation and inhibit cell death, hence promoting tissue growth. How this Yorkie/YAP activation propagates throughout the whole tissue remains unclear. Compared to wild-type controls, depleting Ajuba in the developing wing results in smaller adult wings (Das Thakur et al., 2010; Marie et al., 2003; Rauskolb et al., 2014), similar to Syd knockdown. We asked whether Syd is required for the junctional sequestration of ajuba or Warts

and found that it is not. RNAi depletion of Syd in P/A boundary cells (*ptcGal4>Syd-RNAi*) did not reduce Ajuba protein levels or alter its subcellular localization (Supplemental Figure 1A, B, *N*=22 discs). Similarly, the subcellular localization of Warts in Syd knockdown cells was indistinguishable from wild-type (Supplemental Figure 1A, C*, N=22* discs).

Next, we asked whether Syd/JIP3 acts downstream of Yorkie/YAP. Overexpression of Yorkie/YAP in the developing wing (*nubGAL4>Yki*) resulted in overgrown wing imaginal discs showing moderate to severe tissue folding (37% and 63%, *N=16*, respectively; Figure 3A-C, E and (Huang et al., 2005)). Syd knockdown (*nubGAL4>Yki, Syd-RNAi*) suppressed the severe tissue folds, yielding relatively much smoother tissues (Figure 3A-E). Thus, Yorkie/YAP requires Syd/JIP3 function to fully exert its tissue overgrowth phenotype. In a complementary approach, we activated Yorkie/YAP by repressing Hippo. In contrast to direct Yorkie/YAP overexpression, this approach activates Yorkie/YAP at physiologically relevant levels. We asked whether knocking down Syd in this context would also repress Yorkie/YAP-mediated tissue overgrowth. As expected, Hippo knockdown resulted in larger wings relative to control (Figure 3F, G, L). *Syd-RNAi* suppressed the large wing effect of Hippo inhibition (Figure 3G, H, J, L). Moreover, heterozygosity of two additional independent *Syd* mutant alleles ($syd^{PL00426/+}$ or $syd^{A2/+}$) was sufficient to significantly suppress *Hippo-RNAi* large wing phenotype (Figure 3G, I, L). Finally, western blot analyses showed that *Hippo-RNAi* triggers the upregulation of Syd/JIP3 protein in wing tissues (Figure 3K). We conclude that Syd/JIP3 regulates wing size downstream of Yorkie/YAP.

We sought to delineate the underlying mechanism. We examined the expression levels of two key Hippo signaling transcriptional targets, Cyclin E (CycE) and Diap1 using standard transcriptional reporter lines (CycE-LacZ and diap1-LacZ) (Jones et al., 2000; Zhang et al., 2008). Interestingly, Diap1 and CycE expression levels were indistinguishable between wild-type and *Syd-RNAi*

expressing cells (Figure 4A, B and Supplemental Figure 2E-H). We extended these analyses to include two additional Hippo signaling transcriptional targets *four-jointed* (fj) and *expanded* (Ex) (Cho et al., 2006; Hamaratoglu et al., 2006) and found that Syd knockdown does not affect the expression of *fj* or *Ex* (Supplemental Figure 2A-D, 2I-K). Thus, it is unlikely that Syd/JIP3 controls wing size by regulating the Hippo transcriptional program.

We explored the possibility that Syd/JIP3 controls cellular response to Hippo signaling via a post-translational mechanism and found that it does; although, RNAi knockdown of Syd in the posterior compartment, using *enGAL4* or *HhGAL4,* had no effect on Diap1 expression, immuno-staining experiments using antibodies against Diap1 protein revealed a notable reduction of Diap1 protein levels (Figure 4A-D). In a complementary approach, we performed western blot assays using lysates prepared from these posterior Syd knocked down tissues (*HhGAL4>Syd-RNAi*). Compared to wild-type controls, Syd knockdown in only half of the cells was sufficient to show a reduction of Diap1 protein levels (Figure 4R). Diap1 normally promotes cell survival by antagonizing the pro-apoptotic caspase Dronc (Nedd2-like caspase–FlyBase) (Lee et al., 2011; Wilson et al., 2002). Concordant with a loss of Diap1 protein, Syd knockdown in posterior compartment cells (*HhGAL4>Syd-RNAi*) resulted in ectopic cell death compared to anterior compartment cells within the same tissues using TUNEL assays (Figure 4G, H). These findings strongly argue that Syd/JIP3 promotes wing growth by stabilizing Diap1 activity.

The E3 ubiquitin ligase function of the Diap1 RING finger domain enables Diap1 to degrade not only downstream substrates, but also itself to modulate cell survival (Ryoo et al., 2002; Yoo, 2005; Yoo et al., 2002). Similar to inhibitor of apoptosis (IAP) proteins in vertebrates, Diap1 dimerizes and self-ubiquitinates via its RING domain to trigger its own proteolysis (Feltham et al., 2011; Mace et al., 2008; Rumpf et al., 2011; Silke et al., 2005). Ectopic expression experiments have shown that inhibition of the RING domain via point mutations or deletions (RINGΔ) results in a

significant stabilization of not only the mutant protein but also endogenous wild-type Diap1, consistent with Diap1 dimerization (Wilson et al., 2002; Yokokura et al., 2004). RING domain defective *diap1* mutants are homozygous lethal but heterozygous viable, presumably because RINGΔ–wild-type Diap1 heterodimers still retain some ability to inhibit Dronc and promote cell survival (Lisi et al., 2000; Wilson et al., 2002; Yokokura et al., 2004). We asked to what extent diap1 RINGΔ heterozygosity restores Diap1 protein levels in Syd/JIP3 knocked down cells.

We took advantage of a heterozygous viable *diap1* RINGΔ mutation [$diap1^{(33\text{-}1s)}$] (Wilson et al., 2002) and asked whether its heterozygosity rescues Diap1 in Syd/JIP3-depleted wings. Heterozygosity of the $diap1^{(33\text{-}1s)}$ allele [$diap1^{(33\text{-}1s)/+}$] restored Diap1 protein levels in *Syd-RNAi* expressing cells (*enGAL4>Syd-RNAi,* $diap1^{(33\text{-}1)s/+}$, Figure 4C-F; 71%, *N=14*) and correspondingly rescued wing size (Figure 4I-M, O, Q). Thus, Syd/JIP3 controls tissues size via Diap1.

Also, given the loss of Diap1 protein in Syd/JIP3-depleted tissues and the resulting ectopic cell death, this would elevate Dronc activity. We predicted that Syd/JIP3-depleted tissues would be sensitive to Dronc dosage such that a partial reduction of Dronc function (Dronc haploinsufficiency, $dronc^{51/+}$) will be sufficient to restore wing size to some extents. Indeed, heterozygosity of a *dronc* null allele ($dronc^{51}$) rescued wing size in *Syd-RNAi* animals (Figure 4I, K, L, N, P, Q).

Finally, we turned to HEK-293 cells to assess whether Syd/JIP3 similarly regulates cell survival and cell growth in mammalian cells. RNAi knockdown of JIP3 inhibited the growth of HEK-293 cells and caused ectopic cell death in flow cytometric assays (Figure 4S-U), mimicking Syd/JIP3 knockdown in *Drosophila*. Collectively, these findings highlight a novel and conserved Syd/JIP3 growth control mechanism. Our data indicate that Syd/JIP3 controls tissue size downstream of the Yorkie/YAP by regulating Diap1 protein turnover, hence modulating cell survival and ultimately tissue size.

Discussion

Our understanding of the molecular underpinnings of organ size regulation is incomplete. Genetic screens in *Drosophila* imaginal discs have led to the identification of Hippo signaling as a central and evolutionarily conserved growth control mechanism. More recently Willsey and colleagues reported that in *Drosophila*, developmentally encoded signals trigger JNK activation at the posterior-anterior boundary of the developing wing. This localized JNK activity, broadly inhibits Hippo signaling to promote tissue-wide cell proliferation, resulting in a properly sized adult wing (Willsey et al., 2016). Here we show that Syd/JIP3 regulates wing size downstream of Yorkie by controlling Diap1 protein turnover.

Direct activation of Yorkie/YAP potently triggers tissue overgrowth in vertebrates and *Drosophila*. Syd knockdown partly suppresses Yorkie/YAP-mediated tissue overgrowth. The moderate effect is likely because direct activation of Yorkie/YAP is so potent that the resulting ectopic cell proliferation masks the impact of *Syd-RNAi/Diap1*-mediated cell death in these tissues. Consistent with this, depletion of Syd protein under three independent experimental conditions (*Syd-RNAi* or Syd haploinsufficiency using $Syd^{PL00426}$ or Syd^{A2} loss of function alleles) suppressed the large wing phenotype resulting from Hippo knockdown. In addition, activation of Yorkie/YAP unregulated Syd/JIP3 protein. These findings are consistent with Syd/JIP3 acting downstream of Yorkie/YAP signaling in wing size regulation.

Syd/JIP3 regulates wing size by controlling Diap1 protein stability. Inhibition of Syd/JIP3 decreases Diap1 protein levels and correspondingly triggers ectopic cell death. Similar to *Syd-RNAi*, expression of *Diap1-RNAi* in P/A cells is sufficient to reduce adult wing size (Supplemental Figure 4). Partial restoration of Diap1 rescues the small wing effect of Syd/JIP3 inhibition. The partial rescue may reflect an incomplete restoration of Diap1 protein and/or that the re-established

pool of Diap1 is only partly effective at inhibiting cell death. We cannot rule out the possibility that Syd/JIP3 tissue size regulation involves additional Diap1-independent mechanisms.

The observation that Diap1 RINGΔ heterozygosity restores Diap1 protein levels in Syd/JIP3 knockdown cells supports the notion that Syd/JIP3 normally stabilizes Diap1 by protecting it from proteolytic degradation.

Ectopic cell death is the primary mechanism underlying the reduced growth of Syd knockdown *Drosophila* tissues and human cells. We did not detect a decrease of proliferative capacity in *Syd-RNAi* expressing *Drosophila* tissues compared to wild-type controls (Supplemental Figure 3).

This study has identified Syd/JIP3 as a novel size regulator downstream of Hippo. It is tempting to speculate that Syd/JIP3 regulation of Diap1 likely represents a dynamic developmental tuning mechanism for scaling tissues' response to Hippo signaling or Diap1 effectors. In support of this notion, *Syd/JIP3* is expressed at higher levels during the rapid growth phase (72-96 hours after egg laying-AEL) and progressively drops in third-instar (120-150 hours AEL) when growth slows down (Supplemental Figure 5). High levels of Syd/JIP3 would stabilize Diap1, enabling robust growth during the rapid growth phase. The decline of Syd/JIP3 transcription later in development would scale growth down by targeting Diap1 for degradation, hence allowing some cell death to occur to finalize tissue size. Additional significance can be derived from the fact that our findings provide potential mechanistic insights into the recent and perplexing link between *JIP3* mutations and organ size defects in mammals, including humans where de novo *JIP3* variants are associated with microcephaly (Kelkar et al., 2003; Platzer et al., 2019).

Acknowledgment

We thank A. Bergmann, G Halder, T. Xu, H. Steller, M. Baylies and D. Pan for antibodies and fly stocks. We also thank Bloomington Drosophila Stock Center for fly lines. We also thank M. Kroll for comments on the manuscript.

Reference

Bowman, A.B., Kamal, A., Ritchings, B.W., Philp, A.V., McGrail, M., Gindhart, J.G., Goldstein, L.S., 2000. Kinesin-dependent axonal transport is mediated by the sunday driver (SYD) protein. Cell 103, 583-594.
Bryant, P.J., Levinson, P., 1985. Intrinsic growth control in the imaginal primordia of Drosophila, and the autonomous action of a lethal mutation causing overgrowth. Dev Biol 107, 355-363.
Caswell, P.T., Dickens, M., 2018. JIP3 localises to exocytic vesicles and focal adhesions in the growth cones of differentiated PC12 cells. Mol Cell Biochem 444, 1-13.
Chabu, C., Xu, T., 2014. Oncogenic Ras stimulates Eiger/TNF exocytosis to promote growth. Development 141, 4729-4739.
Cho, E., Feng, Y., Rauskolb, C., Maitra, S., Fehon, R., Irvine, K.D., 2006. Delineation of a Fat tumor suppressor pathway. Nat Genet 38, 1142-1150.
Choudhary, B., Kamak, M., Ratnakaran, N., Kumar, J., Awasthi, A., Li, C., Nguyen, K., Matsumoto, K., Hisamoto, N., Koushika, S.P., 2017. UNC-16/JIP3 regulates early events in synaptic vesicle protein trafficking via LRK-1/LRRK2 and AP complexes. PLoS Genet 13, e1007100.
Das Thakur, M., Feng, Y., Jagannathan, R., Seppa, M.J., Skeath, J.B., Longmore, G.D., 2010. Ajuba LIM proteins are negative regulators of the Hippo signaling pathway. Curr Biol 20, 657-662.
Davis, R.J., 2000. Signal transduction by the JNK group of MAP kinases. Cell 103, 239-252.
Day, S.J., Lawrence, P.A., 2000. Measuring dimensions: the regulation of size and shape. Development 127, 2977-2987.
Dong, J., Feldmann, G., Huang, J., Wu, S., Zhang, N., Comerford, S.A., Gayyed, M.F., Anders, R.A., Maitra, A., Pan, D., 2007. Elucidation of a universal size-control mechanism in Drosophila and mammals. Cell 130, 1120-1133.
Edwards, S.L., Yu, S.C., Hoover, C.M., Phillips, B.C., Richmond, J.E., Miller, K.G., 2013. An organelle gatekeeper function for Caenorhabditis elegans UNC-16 (JIP3) at the axon initial segment. Genetics 194, 143-161.
Feltham, R., Bettjeman, B., Budhidarmo, R., Mace, P.D., Shirley, S., Condon, S.M., Chunduru, S.K., McKinlay, M.A., Vaux, D.L., Silke, J., Day, C.L., 2011. Smac mimetics activate the E3 ligase activity of cIAP1 protein by promoting RING domain dimerization. J Biol Chem 286, 17015-17028.
Fristrom, D., Chihara, C., 1978. The mechanism of evagination of imaginal discs of Drosophila melanogaster. V. Evagination of disc fragments. Dev Biol 66, 564-570.
Garcia-Bellido, A., 1975. Genetic control of wing disc development in Drosophila. Ciba Found Symp 0, 161-182.
Garcia-Bellido, A., Merriam, J.R., 1971. Parameters of the wing imaginal disc development of Drosophila melanogaster. Dev Biol 24, 61-87.
Gowrishankar, S., Wu, Y., Ferguson, S.M., 2017. Impaired JIP3-dependent axonal lysosome transport promotes amyloid plaque pathology. J Cell Biol 216, 3291-3305.
Hacker, U., Nystedt, S., Barmchi, M.P., Horn, C., Wimmer, E.A., 2003. piggyBac-based insertional mutagenesis in the presence of stably integrated P elements in Drosophila. Proc Natl Acad Sci U S A 100, 7720-7725.
Hamaratoglu, F., Willecke, M., Kango-Singh, M., Nolo, R., Hyun, E., Tao, C., Jafar-Nejad, H., Halder, G., 2006. The tumour-suppressor genes NF2/Merlin and Expanded act through Hippo signalling to regulate cell proliferation and apoptosis. Nat Cell Biol 8, 27-36.

Hariharan, I.K., 2015. Organ Size Control: Lessons from Drosophila. Dev Cell 34, 255-265.
Huang, J., Wu, S., Barrera, J., Matthews, K., Pan, D., 2005. The Hippo signaling pathway coordinately regulates cell proliferation and apoptosis by inactivating Yorkie, the Drosophila Homolog of YAP. Cell 122, 421-434.
Irvine, K.D., Harvey, K.F., 2015. Control of organ growth by patterning and hippo signaling in Drosophila. Cold Spring Harb Perspect Biol 7.
Jia, J., Zhang, W., Wang, B., Trinko, R., Jiang, J., 2003. The Drosophila Ste20 family kinase dMST functions as a tumor suppressor by restricting cell proliferation and promoting apoptosis. Genes Dev 17, 2514-2519.
Jones, L., Richardson, H., Saint, R., 2000. Tissue-specific regulation of cyclin E transcription during Drosophila melanogaster embryogenesis. Development 127, 4619-4630.
Katsuyama, T., Comoglio, F., Seimiya, M., Cabuy, E., Paro, R., 2015. During Drosophila disc regeneration, JAK/STAT coordinates cell proliferation with Dilp8-mediated developmental delay. Proc Natl Acad Sci U S A 112, E2327-2336.
Kelkar, N., Delmotte, M.H., Weston, C.R., Barrett, T., Sheppard, B.J., Flavell, R.A., Davis, R.J., 2003. Morphogenesis of the telencephalic commissure requires scaffold protein JNK-interacting protein 3 (JIP3). Proc Natl Acad Sci U S A 100, 9843-9848.
Kelkar, N., Gupta, S., Dickens, M., Davis, R.J., 2000. Interaction of a mitogen-activated protein kinase signaling module with the neuronal protein JIP3. Mol Cell Biol 20, 1030-1043.
Lee, T.V., Fan, Y., Wang, S., Srivastava, M., Broemer, M., Meier, P., Bergmann, A., 2011. Drosophila IAP1-mediated ubiquitylation controls activation of the initiator caspase DRONC independent of protein degradation. PLoS Genet 7, e1002261.
Lisi, S., Mazzon, I., White, K., 2000. Diverse domains of THREAD/DIAP1 are required to inhibit apoptosis induced by REAPER and HID in Drosophila. Genetics 154, 669-678.
Mace, P.D., Linke, K., Feltham, R., Schumacher, F.R., Smith, C.A., Vaux, D.L., Silke, J., Day, C.L., 2008. Structures of the cIAP2 RING domain reveal conformational changes associated with ubiquitin-conjugating enzyme (E2) recruitment. J Biol Chem 283, 31633-31640.
Mandaravally Madhavan, M., Schneiderman, H.A., 1977. Histological analysis of the dynamics of growth of imaginal discs and histoblast nests during the larval development ofDrosophila melanogaster. Wilehm Roux Arch Dev Biol 183, 269-305.
Marie, H., Pratt, S.J., Betson, M., Epple, H., Kittler, J.T., Meek, L., Moss, S.J., Troyanovsky, S., Attwell, D., Longmore, G.D., Braga, V.M., 2003. The LIM protein Ajuba is recruited to cadherin-dependent cell junctions through an association with alpha-catenin. J Biol Chem 278, 1220-1228.
Martin, F.A., Herrera, S.C., Morata, G., 2009. Cell competition, growth and size control in the Drosophila wing imaginal disc. Development 136, 3747-3756.
Milan, M., Campuzano, S., Garcia-Bellido, A., 1996. Cell cycling and patterned cell proliferation in the wing primordium of Drosophila. Proc Natl Acad Sci U S A 93, 640-645.
Oh, H., Irvine, K.D., 2008. In vivo regulation of Yorkie phosphorylation and localization. Development 135, 1081-1088.
Pagliarini, R.A., Xu, T., 2003. A genetic screen in Drosophila for metastatic behavior. Science 302, 1227-1231.
Pan, D., 2007. Hippo signaling in organ size control. Genes Dev 21, 886-897.
Platzer, K., Sticht, H., Edwards, S.L., Allen, W., Angione, K.M., Bonati, M.T., Brasington, C., Cho, M.T., Demmer, L.A., Falik-Zaccai, T., Gamble, C.N., Hellenbroich, Y., Iascone, M., Kok, F., Mahida, S., Mandel, H., Marquardt, T., McWalter, K., Panis, B., Pepler, A., Pinz, H., Ramos, L., Shinde, D.N., Smith-Hicks, C., Stegmann, A.P.A., Stobe, P., Stumpel, C., Wilson, C., Lemke, J.R., Di Donato, N., Miller, K.G., Jamra, R., 2019. De Novo Variants in MAPK8IP3 Cause Intellectual Disability with Variable Brain Anomalies. Am J Hum Genet 104, 203-212.

Rauskolb, C., Sun, S., Sun, G., Pan, Y., Irvine, K.D., 2014. Cytoskeletal tension inhibits Hippo signaling through an Ajuba-Warts complex. Cell 158, 143-156.
Rumpf, S., Lee, S.B., Jan, L.Y., Jan, Y.N., 2011. Neuronal remodeling and apoptosis require VCP-dependent degradation of the apoptosis inhibitor DIAP1. Development 138, 1153-1160.
Ryoo, H.D., Bergmann, A., Gonen, H., Ciechanover, A., Steller, H., 2002. Regulation of Drosophila IAP1 degradation and apoptosis by reaper and ubcD1. Nat Cell Biol 4, 432-438.
Sabino, D., Brown, N.H., Basto, R., 2011. Drosophila Ajuba is not an Aurora-A activator but is required to maintain Aurora-A at the centrosome. J Cell Sci 124, 1156-1166.
Silke, J., Kratina, T., Chu, D., Ekert, P.G., Day, C.L., Pakusch, M., Huang, D.C., Vaux, D.L., 2005. Determination of cell survival by RING-mediated regulation of inhibitor of apoptosis (IAP) protein abundance. Proc Natl Acad Sci U S A 102, 16182-16187.
Stocker, H., Hafen, E., 2000. Genetic control of cell size. Curr Opin Genet Dev 10, 529-535.
Sun, G., Irvine, K.D., 2013. Ajuba family proteins link JNK to Hippo signaling. Sci Signal 6, ra81.
Sun, T., Li, Y., Li, T., Ma, H., Guo, Y., Jiang, X., Hou, M., Huang, S., Chen, Z., 2017. JIP1 and JIP3 cooperate to mediate TrkB anterograde axonal transport by activating kinesin-1. Cell Mol Life Sci 74, 4027-4044.
Tabata, T., Eaton, S., Kornberg, T.B., 1992. The Drosophila hedgehog gene is expressed specifically in posterior compartment cells and is a target of engrailed regulation. Genes Dev 6, 2635-2645.
Taylor, M., Alessi, D.R., 2020. Advances in elucidating the function of leucine-rich repeat protein kinase-2 in normal cells and Parkinson's disease. Curr Opin Cell Biol 63, 102-113.
Twitty V. C., S.J.L., 1931. The growth of eyes and limbs transplanted heteroplastically between two species of Amblystoma. J. Exp. Zool. 59, 61-86.
Willsey, H.R., Zheng, X., Carlos Pastor-Pareja, J., Willsey, A.J., Beachy, P.A., Xu, T., 2016. Localized JNK signaling regulates organ size during development. Elife 5.
Wilson, R., Goyal, L., Ditzel, M., Zachariou, A., Baker, D.A., Agapite, J., Steller, H., Meier, P., 2002. The DIAP1 RING finger mediates ubiquitination of Dronc and is indispensable for regulating apoptosis. Nat Cell Biol 4, 445-450.
Worley, M.I., Setiawan, L., Hariharan, I.K., 2013. TIE-DYE: a combinatorial marking system to visualize and genetically manipulate clones during development in Drosophila melanogaster. Development 140, 3275-3284.
Yokokura, T., Dresnek, D., Huseinovic, N., Lisi, S., Abdelwahid, E., Bangs, P., White, K., 2004. Dissection of DIAP1 functional domains via a mutant replacement strategy. J Biol Chem 279, 52603-52612.
Yoo, S.J., 2005. Grim stimulates Diap1 poly-ubiquitination by binding to UbcD1. Mol Cells 20, 446-451.
Yoo, S.J., Huh, J.R., Muro, I., Yu, H., Wang, L., Wang, S.L., Feldman, R.M., Clem, R.J., Muller, H.A., Hay, B.A., 2002. Hid, Rpr and Grim negatively regulate DIAP1 levels through distinct mechanisms. Nat Cell Biol 4, 416-424.
Zecca, M., Basler, K., Struhl, G., 1995. Sequential organizing activities of engrailed, hedgehog and decapentaplegic in the Drosophila wing. Development 121, 2265-2278.
Zhang, L., Ren, F., Zhang, Q., Chen, Y., Wang, B., Jiang, J., 2008. The TEAD/TEF family of transcription factor Scalloped mediates Hippo signaling in organ size control. Dev Cell 14, 377-387.

Competing interests

None

Author Contributions

V.A and C.Y.C designed the research. V.A performed *Drosophila* experiments and analyzed the data together with C.Y.C. G.P.V performed tissue culture experiments. C.Y.C wrote the manuscript.

Figure Legends

Figure 1. Syd/JIP3 regulates adult wing size

(A-D) Representative images showing adult wings from female animals of the indicated genotypes. Wings from *nubGAL4* or *Syd-RNAi* parental lines are shown in (A) and (B), respectively. (C) Image showing the effect of Syd knockdown (*nubGAL4*, *Syd-RNAi*). (D) Image of a pseudo-color overlay of (A) (shown in brown) and (C) (shown in light indigo). (E) Quantification of wing size. For this and all subsequent quantification figures, plotted values indicate the mean ±SD. The number of tissues analyzed (N) per genotype is indicated inside the bar. All experiments were repeated at least twice. *P*-value is computed from a t-test: p-value < 10^{-20} = ******, p-value = 10^{-20}– 10^{-10} = *****, p-value = 10^{-10} –10^{-5} = ****, p-value = 10^{-5} – 10^{-3} = ***, p-value=10^{-3} – 10^{-2} = **, p-value = 0.01 – 0.05 = *, p-value ≥ 0.05 = not significant, ns.

Figure 2. Syd/JIP3 functions downstream of JNK

(A-J) Representative images showing adult wings from female animals of the indicated genotypes. Wing images from control parental fly lines are shown in (A-E). (F-J) Pseudo-color overlay of wing images dissected from *ptcGAL4* control (brown) or from $Syd^{PL00426}/Syd^{A2}$ trans-heterozygote animals (indigo) (F) or animals expressing *Syd-RNAi* (G) or *Bsk-DN* (H) or co-expressing *Syd-*

RNAi and *Bsk-DN* (I) or wild-type *Syd* and *Bsk-DN* (J) all under the control of *ptcGAL4*. (K) Quantification of (A-J).

Figure 3. Syd/JIP3 functions in the Hippo pathway

(A-D) Images of wing imaginal discs from age-controlled animals expressing *RFP* alone (A) or co-expressing *Yorkie* (B and C) or co-expressing *Yorkie* and *Syd-RNAi* (D) under the control of *nubGAL4*. (E) Quantification of (A-D). *Yorkie* overexpression results in overgrown tissues showing severe or moderate tissue folds, 37% and 63% (N=16), respectively. Syd knockdown (*nubGAL4, Yorkie, Syd-RNAi*) suppressed the appearance of tissue folds and yielded tissues with moderate to smooth folding, 56% and 44% (*N*=16), respectively. Severe tissue folding was not detected in (D). (F-J) Representative images showing adult wings from female animals of the indicated genotypes. Compared to *nubGAL4* control wings (F), expression of *Hippo-RNAi* increased wing size (G). *Syd* haploinsufficiency ($Syd^{PL00426/+}$) suppressed the size augmenting effect of *Hippo-RNAi* expression (H). Pseudo-color overlay wing images are shown in (I and J). (I) Wings expressing *Hippo-RNAi* in the absence or presence of Syd haploinsufficiency ($Syd^{PL00426/+}$) are shown in brown and indigo, respectively. (J) Wings expressing *Hippo-RNAi* in the absence or presence of *Syd-RNAi* are shown in brown and indigo, respectively. (K) Western blot image using protein lysate prepared from third instar dissected wing discs expressing *nubGAL4 alone or nubGAL4>Hpo-RNAi*. Blots were stained with anti-JIP3 or anti β-actin (loading control). (L) Quantification of wing size (F-J).

Figure 4. Syd/JIP3 regulates wing size by controlling Diap1 protein turnover

(A-D) Representative images of wing imaginal discs expressing *Syd-RNAi* in the posterior compartment (using *enGAL4* or *HhGAL4*) and stained with antibodies against β-gal to detect Diap1 gene activity from a genomic reporter construct, *Diap1-LacZ* (A, B) or antibodies against Diap1 to

detect Diap1 protein (C, D). (E-H) Representative images of wing imaginal discs expressing *Syd-RNAi* in the posterior compartment in a *diap1*$^{(33\text{-}1s)}$ heterozygote background and stained with anti-Diap1 antibodies (E, F). Representative images of wing imaginal discs expressing *Syd-RNAi* and stained with TUNEL to detect apoptotic cells are shown in (G, H). Blue color represents DAPI stain to mark DNA. A lateral view image section is shown below (H). Green dotted lines denote anterior (A) and posterior (P) compartment boundaries. (I-P) Representative images showing adult wings from female animals of the indicated genotypes. Control wing images are shown in (I) *nubGAL4* alone, (J) *diap1*$^{(33\text{-}1s)}$ heterozygotes, and (K) *dronc*^{51} heterozygotes. Wings derived from *nubGal4* animals expressing *Syd-RNAi* in a wild-type background or under *diap1*$^{(33\text{-}1s)}$ or *dronc*^{51} heterozygosity are shown in L, M, and N. The respective pseudo-color overlay images are shown in (O, P). Brown images are from *nubGAL4, Syd-RNAi* animals. Indigo images are from *nubGAL4, Syd-RNAi* animals heterozygote either for *diap1*$^{(33\text{-}1s)}$ (O) or *dronc*^{51}(P). (Q) Quantification of (I-P). (R) Western blot image using protein lysates derived from dissected third-instar animals expressing *srcRFP* alone (control) or co-expressing *Syd-RNAi* in the posterior compartment using *HhGAL4*. Blots were stained with anti-Diap1 or actin (loading control) antibodies. (S) Western blot image showing JIP3 knockdown in HEK-293 cells. Lysates were prepared from HEK-293 cells treated with scramble control or JIP3-targeted nucleotides. Blots were stained with GAPDH (loading control) or JIP3 antibodies. (T) Graph showing the effect of JIP3 knockdown on HEK-293 cell numbers. (U) Graph showing the comparative proportion of propidium iodide (PI)-positive cells with or without JIP3 knockdown using flow cytometry.

Supplemental Figure 1. Expression and subcellular localization of ajuba and Warts in Syd knockdown cells

(A-C) Lateral section images showing wing imaginal discs containing a genomic rescue construct expressing ajuba tagged with GFP under its own promoter (*Jub-GFP) (Sabino et al., 2011)* and co-expressing *Syd-RNAi* and RFP (shown in blue) under *ptcGAL4*. Tissues were stained with anti-phosphorylated Warts (pWts) antibodies.

Supplemental Figure 2. Transcription of *four-jointed* and *cyclin-E* in Syd knockdown cells

(A-H) Representative images of wing imaginal discs dissected from *four-jointed-LacZ* or *CyclinE-LacZ* reporter lines expressing RFP alone (A, B, E, F) or co-expressing *Syd-RNAi* under *nubGAL4* (C, D, G, H). Tissues are stained with DAPI to detect DNA, β-gal antibodies to detect *four-jointed* (A-D) or *CyclinE* (E-H) gene activities. (I-K) Representative images showing wing imaginal discs co-expressing *Syd-RNAi* and GFP in the posterior compartment with *enGAL4* and stained with anti-Expanded antibodies.

Supplemental Figure 3. Mitotic potential of Syd depleted cells

(A, B) Image showing a wing imaginal disc expressing *Syd-RNAi* under the *HhGAL4* driver and stained with anti-phosphorylated Histone-3 to detect proliferating cells. (C) Quantitation of (A, B). *P*-value (t-test) was 0.78.

Supplemental Figure 4. Effect of Diap1 knockdown on adult wing size

(A, B) Images showing wing imaginal discs dissected from female animals of the indicated genotypes.

(C) Quantification of (A, B).

Supplemental Figure 5. *Syd* gene expression during wing development

Graph showing *Syd/JIP3* expression in wing imaginal discs dissected at the indicated developmental time periods from biological triplicates. *Syd/JIP3* expression was calibrated to *Rp49* expression at each developmental time period. Fold expression changes were established by comparing each time period to the 72-80 hours AEL period. Graph shows mean fold changes in gene expression ± SD.

Figure 1

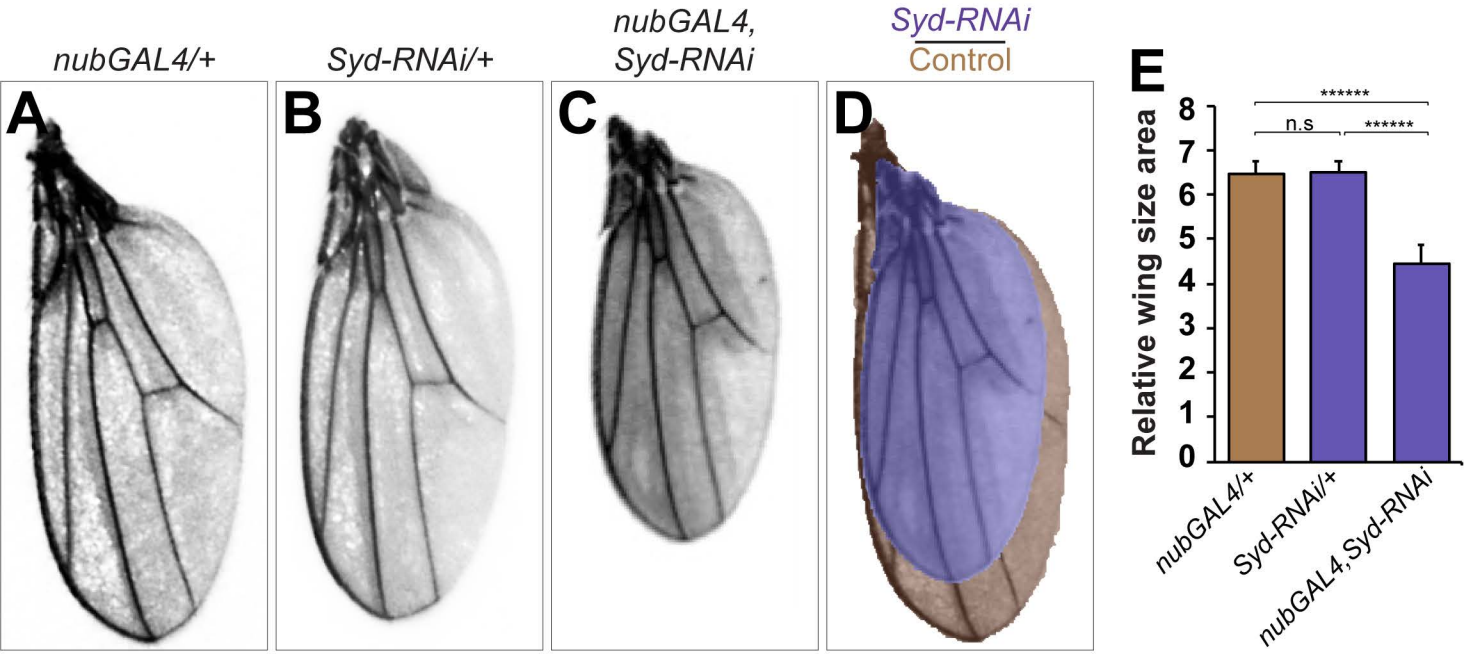
nubGAL4/+
Syd-RNAi/+
nubGAL4,
Syd-RNAi
Syd-RNAi
Control
A
B
C
D
E
Relative wing size area
0
1
2
3
4
5
6
7
8
n.s
******
******
nubGAL4/+
Syd-RNAi/+
nubGAL4,Syd-RNAi

Figure 2

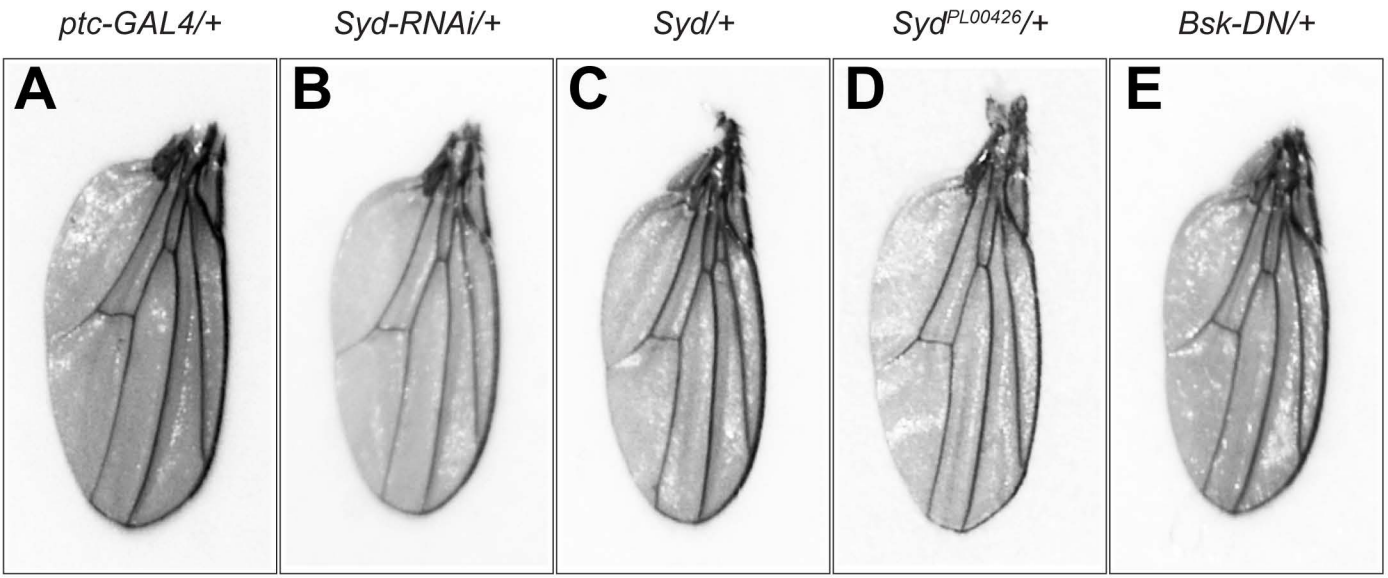
ptc-GAL4/+
Syd-RNAi/+
Syd/+
Syd^PL00426/+
Bsk-DN/+
A
B
C
D
E

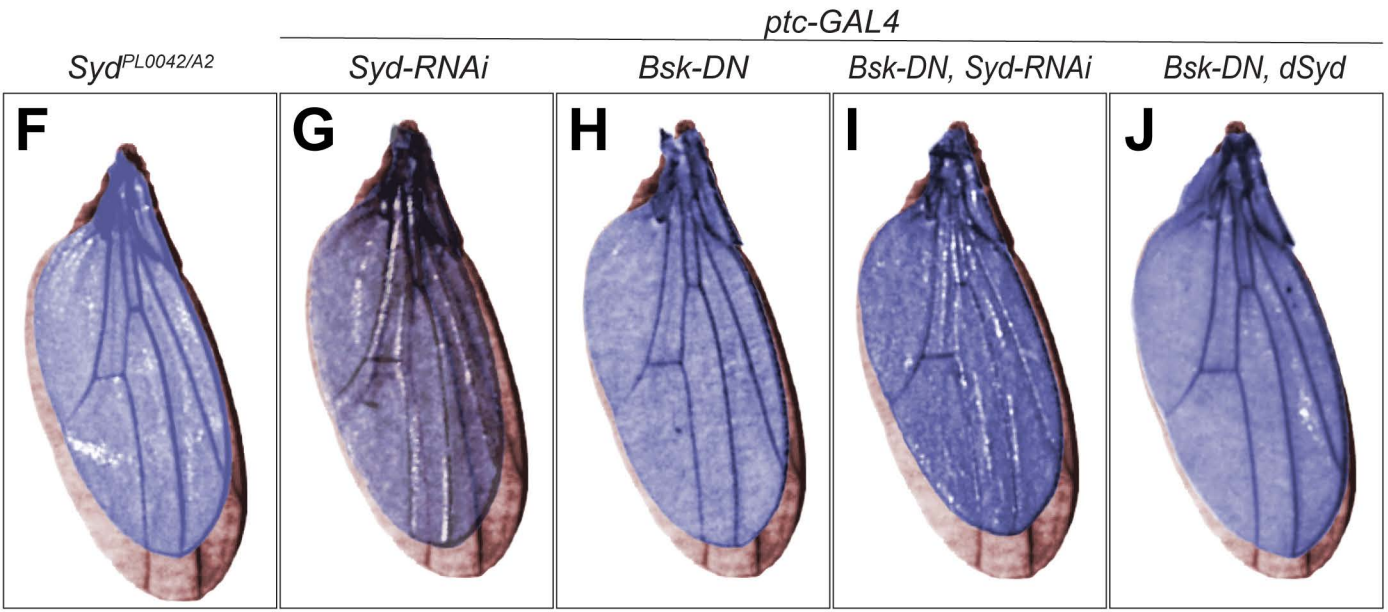
ptc-GAL4
Syd^PL0042/A2
Syd-RNAi
Bsk-DN
Bsk-DN, Syd-RNAi
Bsk-DN, dSyd
F
G
H
I
J

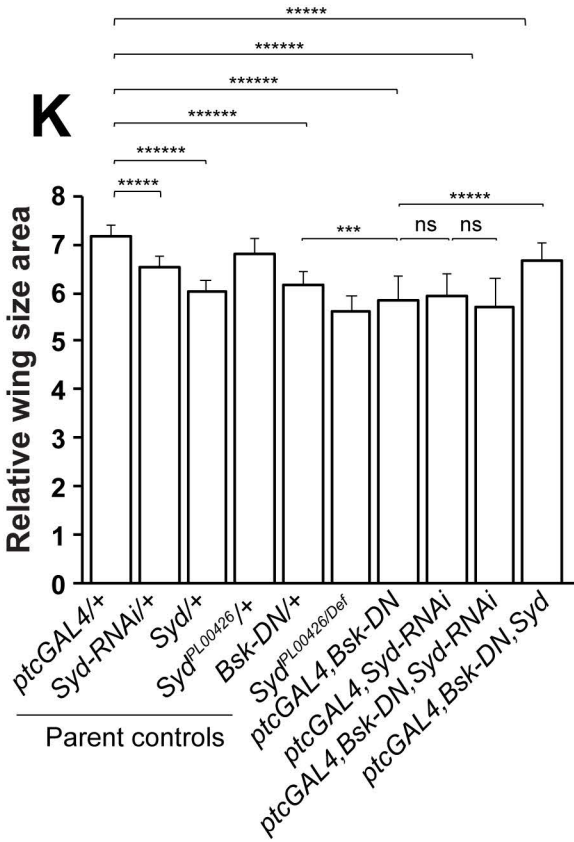
K
Relative wing size area
0
1
2
3
4
5
6
7
8
*****
******
******
******
******
*****
***
ns
ns
*****
ptcGAL4/+
Syd-RNAi/+
Syd/+
Syd^PL00426/+
Bsk-DN/+
Syd^PL00426/Def
ptcGAL4,Bsk-DN
ptcGAL4,Syd-RNAi
ptcGAL4,Bsk-DN,Syd-RNAi
ptcGAL4,Bsk-DN,Syd
Parent controls

Figure 3

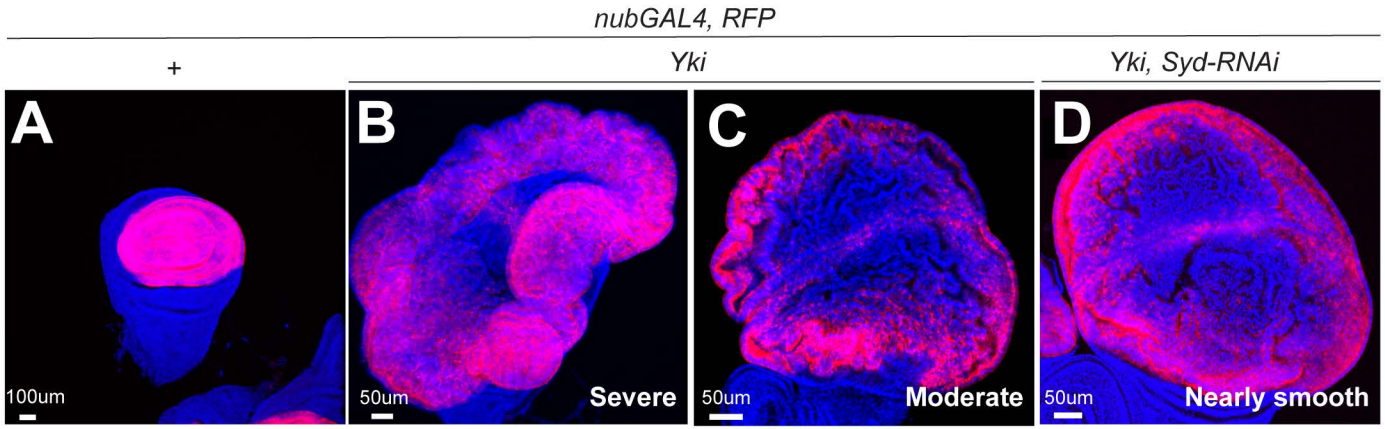
nubGAL4, RFP
+
Yki
Yki, Syd-RNAi
A
B
C
D
100um
50um
Severe
50um
Moderate
50um
Nearly smooth

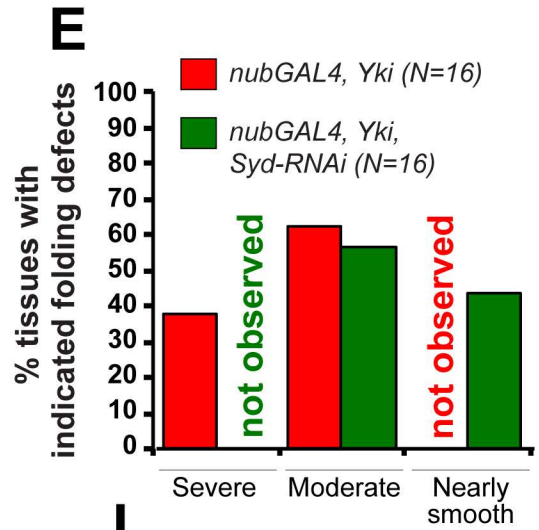
E
nubGAL4, Yki (N=16)
nubGAL4, Yki, Syd-RNAi (N=16)
% tissues with indicated folding defects
100
90
80
70
60
50
40
30
20
10
0
not observed
not observed
Severe
Moderate
Nearly smooth

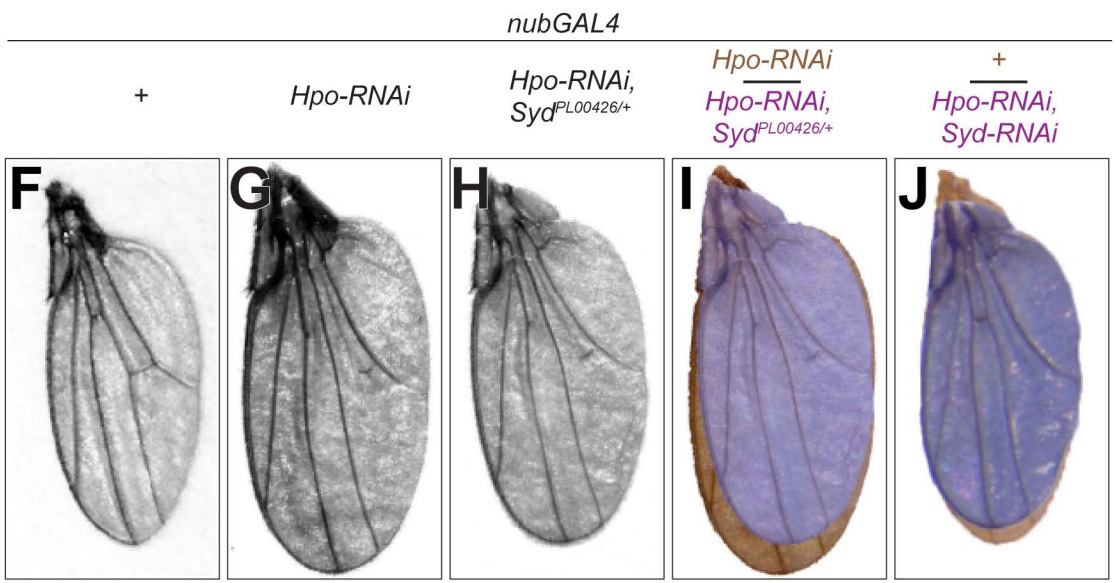
nubGAL4
+
Hpo-RNAi
Hpo-RNAi, Syd$^{PL00426/+}$
Hpo-RNAi
Hpo-RNAi, Syd$^{PL00426/+}$
+
Hpo-RNAi, Syd-RNAi
F
G
H
I
J

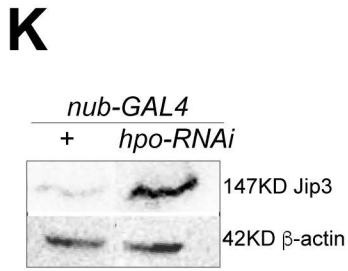
K
nub-GAL4
+
hpo-RNAi
147KD Jip3
42KD β-actin

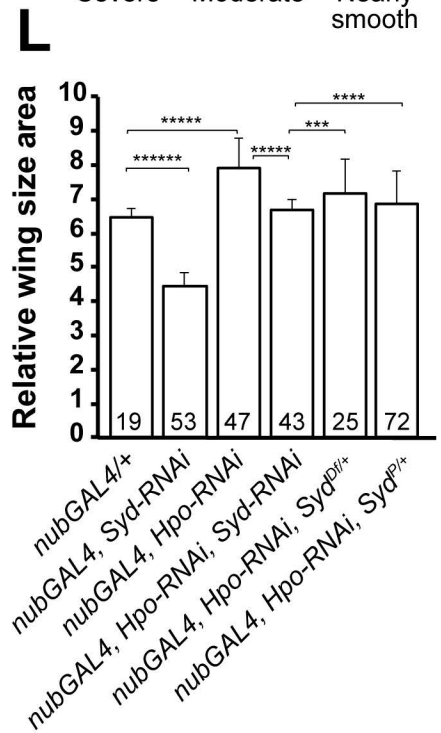
L
Relative wing size area
10
9
8
7
6
5
4
3
2
1
0
******
******
*****
***
****
19
53
47
43
25
72
nubGAL4/+
nubGAL4, Syd-RNAi
nubGAL4, Hpo-RNAi
nubGAL4, Hpo-RNAi, Syd-RNAi
nubGAL4, Hpo-RNAi, Syd$^{Df/+}$
nubGAL4, Hpo-RNAi, Syd$^{P/+}$

Figure 4

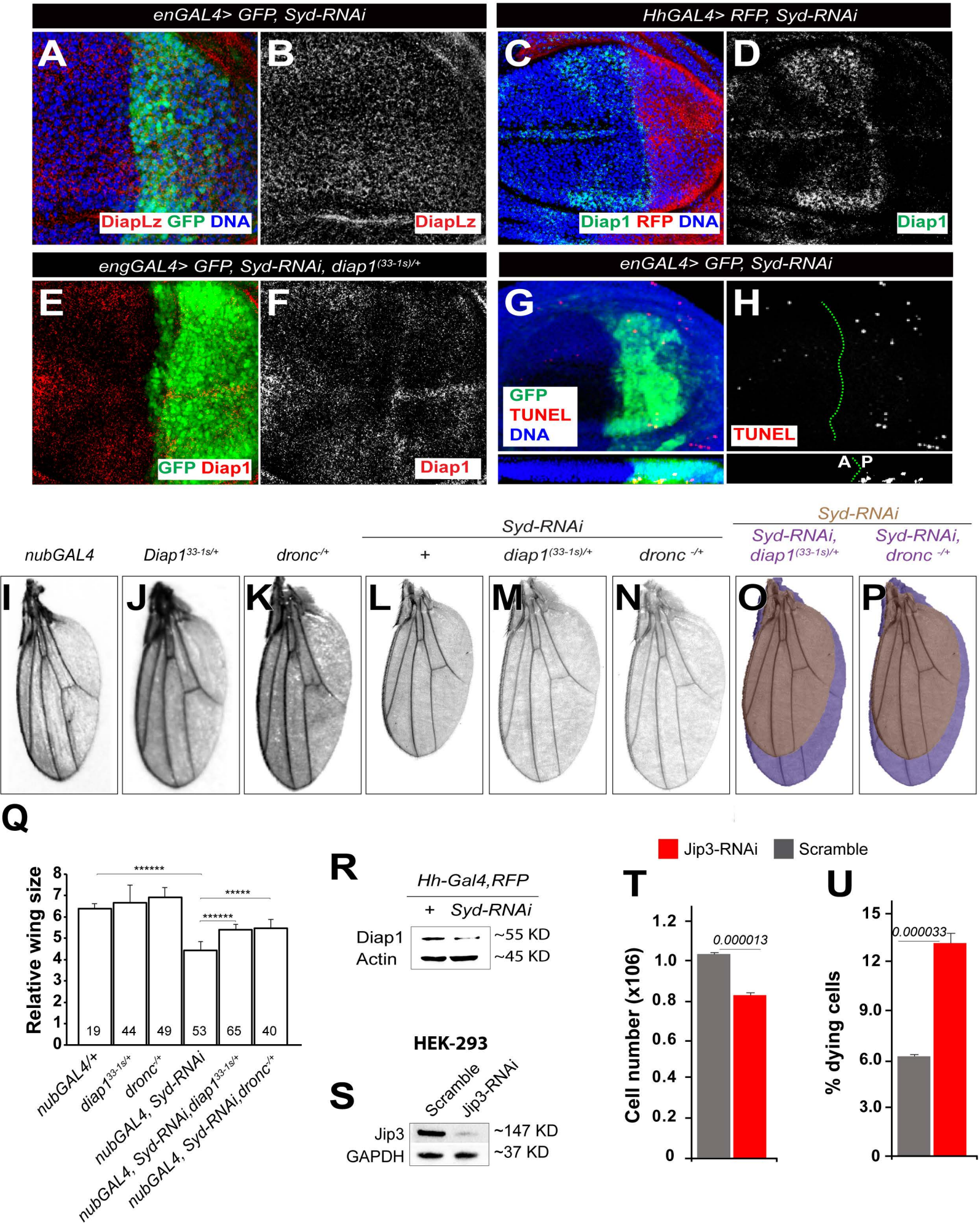
enGAL4> GFP, Syd-RNAi
A
DiapLz GFP DNA
B
DiapLz
HhGAL4> RFP, Syd-RNAi
C
Diap1 RFP DNA
D
Diap1
engGAL4> GFP, Syd-RNAi, diap1(33-1s)/+
E
GFP Diap1
F
Diap1
enGAL4> GFP, Syd-RNAi
G
GFP
TUNEL
DNA
H
TUNEL
A P
nubGAL4
Diap1 33-1s/+
dronc -/+
Syd-RNAi
+
diap1(33-1s)/+
dronc -/+
Syd-RNAi
Syd-RNAi, diap1(33-1s)/+
Syd-RNAi, dronc -/+
I
J
K
L
M
N
O
P
Q
Relative wing size
0
1
2
3
4
5
6
7
8
******
*****
******
19
44
49
53
65
40
nubGAL4/+
diap1 33-1s/+
dronc -/+
nubGAL4, Syd-RNAi
nubGAL4, Syd-RNAi,diap1 33-1s/+
nubGAL4, Syd-RNAi,dronc -/+
R
Hh-Gal4,RFP
+
Syd-RNAi
Diap1
Actin
~55 KD
~45 KD
HEK-293
S
Scramble
Jip3-RNAi
Jip3
GAPDH
~147 KD
~37 KD
Jip3-RNAi
Scramble
T
Cell number (x106)
0
0.2
0.4
0.6
0.8
1.0
1.2
0.000013
U
% dying cells
0
3.0
6.0
9.0
12
15
0.000033

Supplemental Figure 1

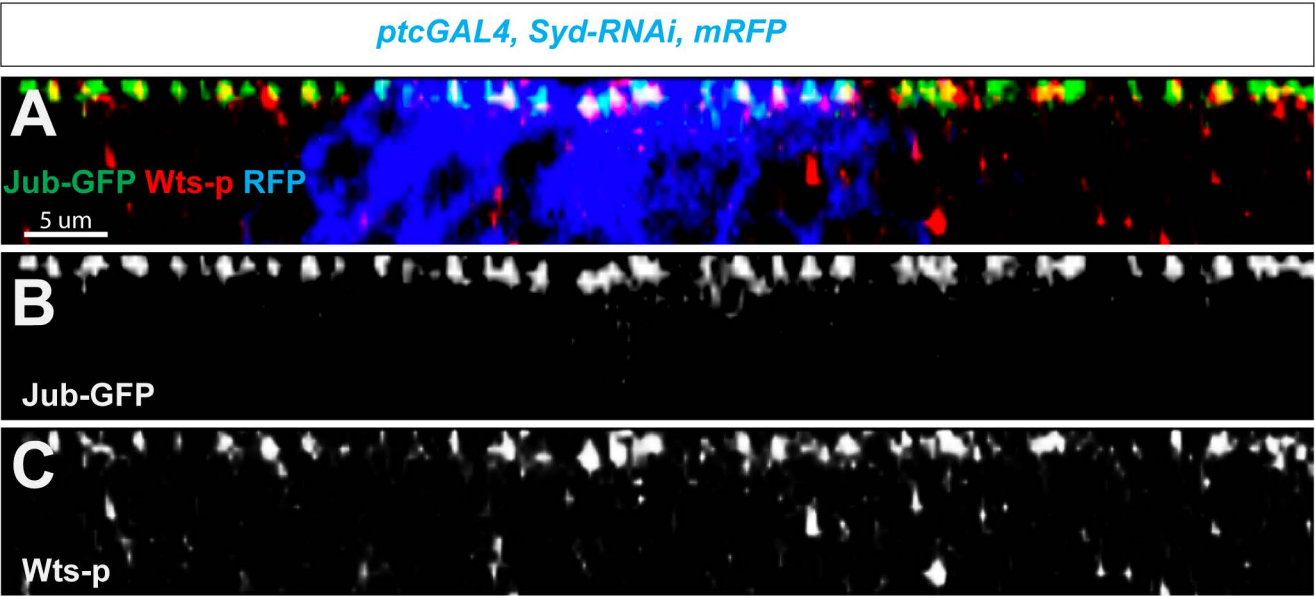

Supplemental Figure 2

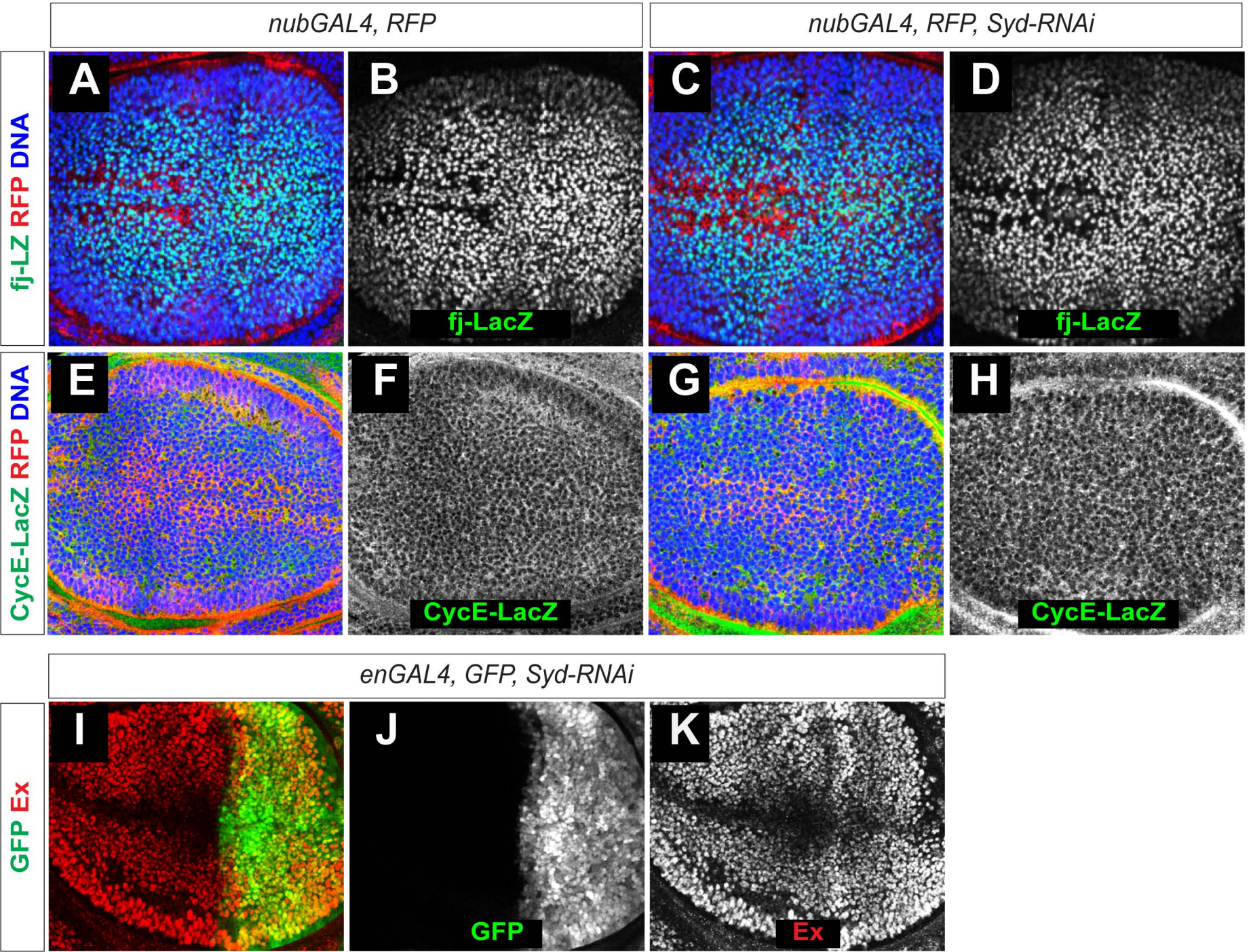

Supplemental Figure 3

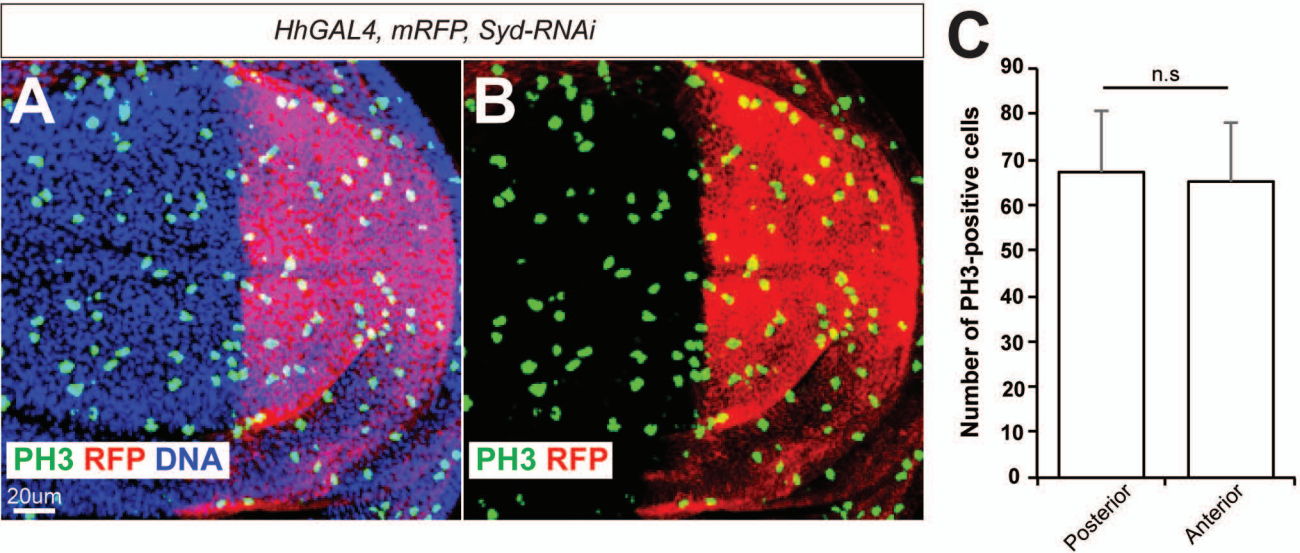

Supplemental Figure 4

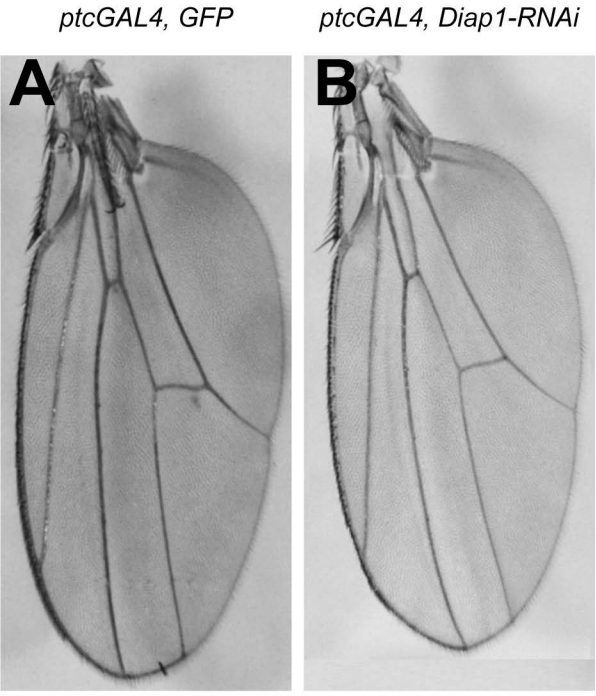

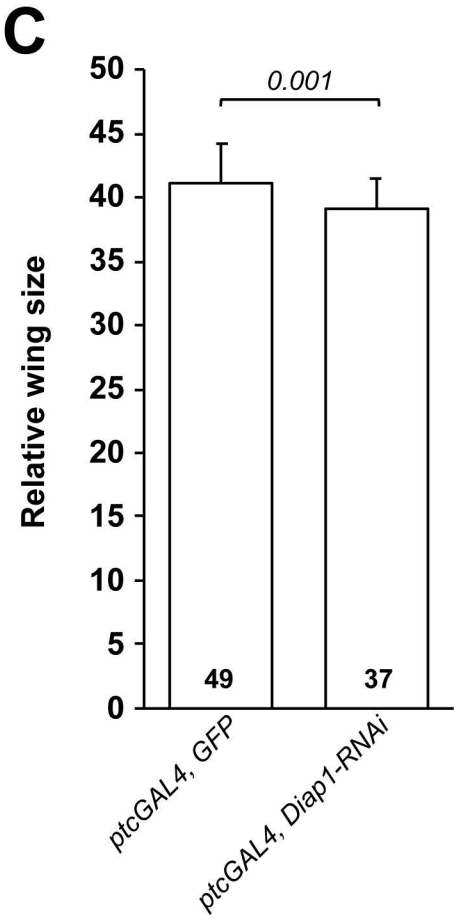
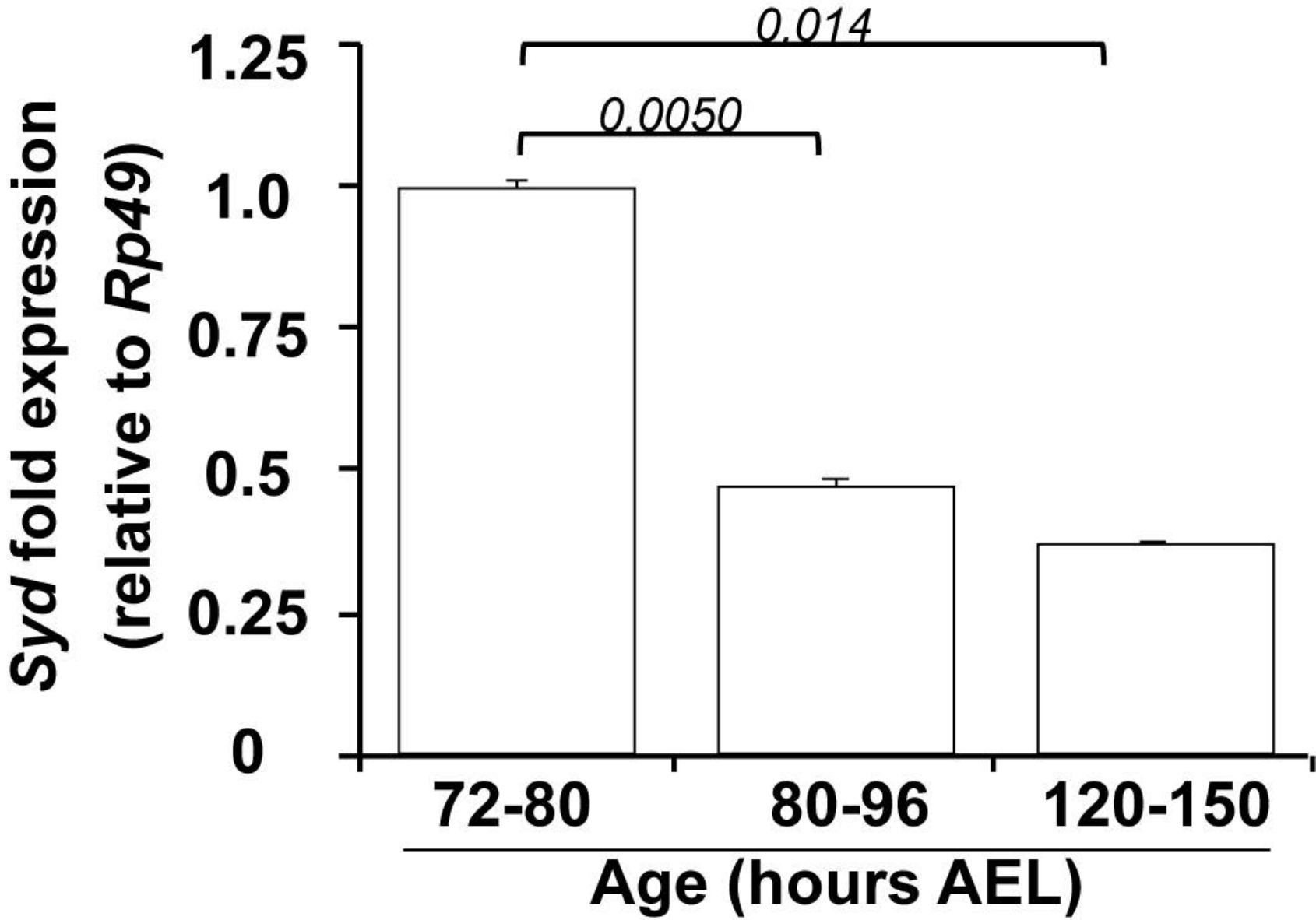
Supplemental Figure 5